

Variations in intra- and extracellular water component differentiation using intrathecal and subcutaneous injections of manganese chloride

Mohammed Salman Shazeeb^{1,2}

¹Radiology, University of Massachusetts Medical School, Worcester, MA, United States, ²Biomedical Engineering, Worcester Polytechnic Institute, Worcester, MA, United States

Introduction: The apparent diffusion coefficient (ADC) of cerebral tissue water decreases during ischemia which has been established by diffusion-weighted nuclear magnetic resonance (NMR) techniques [1-3]. However, it remains unclear whether the ADC change occurs due to changes in the intracellular (IC) space, extracellular (EC) space, or both. Compartment-specific diffusion coefficients using gadolinium have been measured to distinguish between the IC and EC water signals by reducing the longitudinal (T_1) relaxation time of the EC space [4-5]. Manganese (Mn^{2+}), which acts as a calcium analogue, has also shown the potential of separating tissue signal in the rat brain when administered via subcutaneous (SC) injection [6]. However, the extent of differentiation between the compartments was relatively difficult due to the low magnitude of the smaller compartment signal. In this investigation, we explored the differentiation of IC and EC compartments by administering Mn^{2+} directly into the cerebrospinal fluid (CSF) using an intrathecal (IT) injection without any intermediary blood transport. This method can potentially deliver a higher concentration of Mn^{2+} and create substantial water signal to differentiate between the two compartments. This could help shed further light in the understanding of water exchange mechanisms.

Methods: Experiments were carried out using 12 male Sprague Dawley rats weighing 200-450 g. SC injection of $MnCl_2$ was administered in animals ($n=7$) at a dose of 300 mg/kg using 100mM $MnCl_2$. IT injections were performed in animals ($n=5$) using 50 μ L of 25mM $MnCl_2$. All MR imaging was performed at 2.0T. Multi-slice T_1 -weighted (T_1 -WT) MR images (TR/TE = 700/15 ms) were acquired pre-injection and 6, 12, 24, and 48 (IT) or 72 (SC) hrs following Mn^{2+} injection. T_1 relaxation times were measured using an inversion recovery (IR) sequence (TR/TE = 10,000/4.8 ms, 16 inversion time (TI) points ranging from 15 ms to 3300 ms) acquired at the same time points as the T_1 -WT images. Different brain regions of interests (ROIs) were selected (cortex and sub-cortex) from the MRI slices. A mean ROI value from each TI point was calculated and the IR data set was normalized for monoexponential (Eq.1) and biexponential (Eq. 2) analysis using a combination of curve-stripping and non-linear least squares fitting in MATLAB. χ^2 statistics using an F test was used to determine the best fit model.

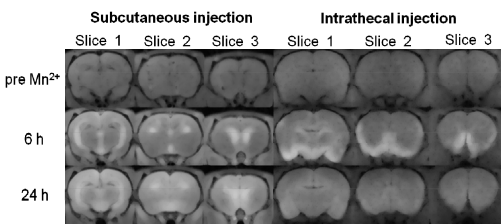


Fig. 1 – Time-course of Mn^{2+} distribution in three corresponding slices of two different rat brains injected with $MnCl_2$ via subcutaneous (100mM, 300mg/kg) and intrathecal (50 μ L 25mM) injections. T_1 -weighted axial

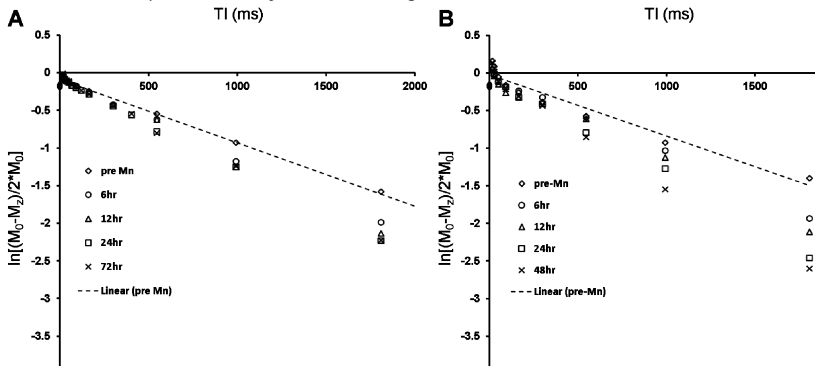


Fig. 2 – Semi-log plots of IR data taken from the cortex region of two rats injected with $MnCl_2$ via (A) subcutaneous, and (B) intrathecal injection. Each graph shows IR data plots at different time points after Mn^{2+} injection. The dotted line shows a monoexponential fit through the IR data set prior to Mn^{2+} administration.

Table 1 – Biexponential fit results for M_{0a} , T_{1a} and T_{1b} (\pm SEM) in the cortex and sub-cortex regions of the rat brain are shown as a function of time after Mn^{2+} administration via SC and IT injections. Due to fitting of normalized data, $M_{0b}=1-M_{0a}$.

		Time after Mn^{2+} SC injection (hrs)				Time after Mn^{2+} IT injection (hrs)			
		6	12	24	72	6	12	24	48
Cortex	M_{0a}	0.95 \pm 0.004 ($n=7$)	0.94 \pm 0.004 ($n=5$)	0.93 \pm 0.002 ($n=7$)	0.95 \pm 0.002 ($n=7$)	0.82 \pm 0.033 ($n=2$)	0.79 \pm 0.069 ($n=2$)	0.82 \pm 0.050 ($n=2$)	0.79 \pm 0.034 ($n=2$)
	T_{1a}	890 \pm 11 ($n=7$)	904 \pm 22 ($n=5$)	850 \pm 10 ($n=7$)	765 \pm 9 ($n=7$)	1186 \pm 260 ($n=2$)	1282 \pm 410 ($n=2$)	1056 \pm 268 ($n=2$)	1095 \pm 245 ($n=2$)
	T_{1b}	27 \pm 0.1 ($n=2$)	28 \pm 10 ($n=2$)	33 \pm 4 ($n=3$)	35 \pm 3 ($n=2$)	43 \pm 9 ($n=2$)	35 \pm 4 ($n=2$)	36 \pm 2 ($n=2$)	44 \pm 5 ($n=2$)
Sub-cortex	M_{0a}	0.93 \pm 0.004 ($n=7$)	0.92 \pm 0.007 ($n=5$)	0.94 \pm 0.004 ($n=7$)	0.91 \pm 0.006 ($n=7$)	0.72 \pm 0.024 ($n=2$)	0.71 \pm 0.045 ($n=2$)	0.66 \pm 0.025 ($n=2$)	0.65 \pm 0.037 ($n=2$)
	T_{1a}	747 \pm 8 ($n=7$)	702 \pm 23 ($n=5$)	621 \pm 11 ($n=7$)	559 \pm 8 ($n=7$)	999 \pm 193 ($n=2$)	1131 \pm 398 ($n=2$)	871 \pm 118 ($n=2$)	977 \pm 132 ($n=2$)
	T_{1b}	21 ($n=1$)	31 ($n=1$)	29 \pm 5 ($n=4$)	47 \pm 12 ($n=2$)	84 \pm 34 ($n=2$)	55 \pm 15 ($n=2$)	98 \pm 32 ($n=2$)	80 \pm 28 ($n=2$)

combined with diffusion measurements, could allow separate measurements of the corresponding component ADCs under both normal and pathological conditions.

References: [1] Wesbey *et al.* (1984). *Invest Radiol* **19**: 491-498; [2] Le Bihan *et al.* (1986). *Radiol* **161**: 401-407; [3] Moseley *et al.* (1990). *Magn Reson Med* **14**: 330-346; [4] Silva *et al.* (2002). *Magn Reson Med* **48**: 826-837; [5] Silva *et al.* (2002). *J Magn Reson* **156**: 52-63; [6] Shazeeb *et al.* (2013) *Proc Int Soc Mag Reson Med* **21**:1259.

$$M_z(t) = M_0(1 - b \cdot e^{\frac{-t}{T_1}}) \quad [\text{Eq. 1}]$$

$$M_z(t) = M_{0a}(1 - b \cdot e^{\frac{-t}{T_{1a}}}) + M_{0b}(1 - b \cdot e^{\frac{-t}{T_{1b}}}) \quad [\text{Eq. 2}]$$

Results and Discussion: Within 6 hrs, T_1 -WT signal enhancement was apparent in the three brain slices of both rats (Fig. 1). The SC injected rat displayed enhancement in the ventricle regions of the brain which gradually spread to the sub-cortex and cortex regions. Mn^{2+} administered via the SC route diffused into the bloodstream and entered the CSF via the choroid plexus and diffused in the proximity of the ventricles. The IT injected rat displayed enhancement in the base of the brain which is consistent with the location of the needle when performing the IT injection. Mn^{2+} spread from the base to the sub-cortex and cortex regions of the brain over time. The IR data sets from both SC and IT injected rats display a biexponential behavior after Mn^{2+} administration. The IT injected rat exhibited a greater extent of differentiation than the SC injected rat (Fig. 2). Table 1 lists the average fit values for M_{0a} , T_{1a} and T_{1b} from the rats that showed a significant fit result. Between the two modes of injection, ANOVA test for mixed models showed a significant difference between the water volume fraction M_{0a} ($P<0.003$) indicating that the Mn^{2+} transport mechanism upon entry to the brain is different for the two cases. There was also a significant effect of time point after SC Mn^{2+} injection ($P < 0.0001$) on the reduction of the long T_1 relaxation times (T_{1a}) in the cortex and sub-cortex regions. The sub-cortex T_{1a} was also significantly less than that of the cortex at all time points for SC injected rat indicating greater Mn^{2+} uptake in the sub-cortex region. The IT injected rat did not show a significant effect of time or ROI on any of the fit parameters. For both cases, T_{1b} and M_{0a} did not show a significant difference between time points or ROIs. The association of T_{1a} with the larger volume fraction, M_{0a} , and T_{1b} with the smaller volume fraction, M_{0b} , occurred with IT injection as was observed with SC [6].

Conclusion: Mn^{2+} injected via SC and IT routes appear to affect the water compartment signals significantly with the IT injected rats exhibiting a stronger differentiation (~75:25) than SC injected rats (~95:5). This might indicate that relaxography with IT route administered Mn^{2+} , when